2×40 Gb/s OCDM using superstructure fiber Bragg gratings en/decoder

Xiaogang Chen (陈小刚), Dexiu Huang (黄德修), Xiuhua Yuan (元秀华), and Ge Xia (夏 舸)

Department of Optoelectronic Engineering and Wuhan National Laboratory for Optoelctrionics,
Huazhong University of Science and Technology, Wuhan 430074

Received August 10, 2005

A 7-chip, 280 Gb/s optical code-division multiplexing (OCDM) system incorporating quaternary phase coding and decoding superstructured fiber Bragg gratings (SSFBGs) is experimentally demonstrated. Only ordinary phase masks and sub-micrometer precision are needed to fabricate the encoding and decoding SSFBGs. Interchannel interference noise is also considered and evaluated, 2-channel 40 (Gb/s)/channel (2 × 40 Gb/s) signal transmission is demonstrated.

OCIS codes: 060.4230, 050.5080, 070.5010.

Optical code-division multiplexing (OCDM) provides unique attributes such as all-optical processing, asynchronous transmission, flexible capacity, high information security, and so on[1]. A key issue within the OCDM system relates to how to reliably generate and recognize appropriate code sequences. Several approaches for generating optical code signals have been reported to date, including arrays of optical fiber delay line[2], planar lightwave circuits (PLCs)[3], arrayed waveguide gratings (AWGs)[4], and fiber grating based devices such as fiber Bragg gratings (FBGs)[5,6]. Recently, superstructured fiber Bragg grating (SSFBG) technology has emerged as an attractive and highly flexible route to produce high performance, and potentially low-cost, code generation and recognition components[7]. The bipolar SSFBGs were fabricated using particular "continuous grating writing" technique[8]. In this technique, a translation stage with sub-nanometer precision is required for accurate fiber or phase mask displacement control.

In this letter, we present an experimental demonstration of 2-channel 40 (Gb/s)/channel (2×40 Gb/s) OCDM system employing 4-phase pulse pattern generation and recognition. The 7-chip 280 Gb/s encoders and decoders are fabricated using equivalent phase shift method[9]. Only ordinary phase masks and sub-micrometer precision in control are needed.

Figure 1 is a diagram of the 2-channel OCDM system that allows multi-channel experiments. A 40-GHz tunable mode-locked laser diode (MLLD) generated 1.3-ps pulse train, the pulse stream was then split using a 3-dB coupler and reflected off from two encoder gratings Q_1, Q_2 to generate 2 separate coded channels. Individual channel signal powers were equalized by variable attenuators and recombined in a 3-dB coupler. After being amplified by erbium-doped fiber amplifier (EDFA), the encoded signals were then fed onto decoder Q_1^*. The individual gratings were denoted by Q_1, Q_2 and Q_1^*, where the subscripts related to a specific code, and asterisk indicated the associated matched filter. The decoder SSFBG Q_1^* operated as a matched filter was used to recognize the encoded sequence. Both SSFBGs were strain-tuned in order to finely match their operating wavelengths. The output pulse of the decoder was measured and analyzed using both a fast photodiode (PD)/scope (∼ 55 GHz bandwidth) and an autocorrelator (< 100 fs resolution), Tektronix CSA8000B with optical module and APE autocorrelator were employed. Several EDFAs were included at various points in the system to restore the signal power, and a polarization controller (PC) was needed before the autocorrelator.

The encoders Q_1, Q_2 and decoder Q_1^* used within our experiments are 4-phase shift SSFBGs. The intensity reflectivity profiles of the encoder gratings Q_1 and Q_2 are shown in Fig. 2. The codes used are members of the Family A sequences. Compared with bipolar and unipolar coding, quaternary coding is known to provide codes with more desirable cross-correlation characteristics[10]. Each grating containing 7 chips has a uniform amplitude refractive index level along its length but in which discrete jumps in phase (0, $\pi/2$, π, or $3\pi/2$) are written into the grating at the boundaries of adjacent spatial chips. The total length of the grating is 2.59 mm, and the individual chip length is 0.37 mm. This corresponds to a total code and chip duration of 25.1 and 3.6 ps, respectively. The gratings are weakly reflecting SSFBGs (reflectivity typically < 20%). The SSFBG based approach relies upon the fact that the impulse response function of a weakly reflecting SSFBG follows directly the profile of the refractive-index superstructure function

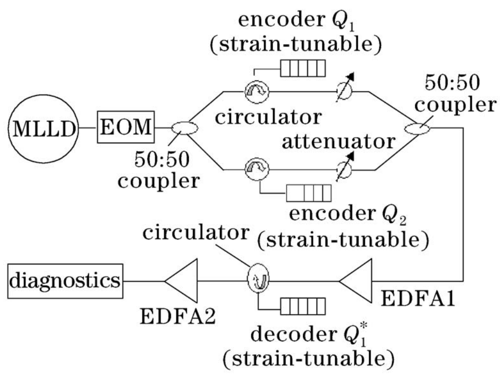

Fig. 1. Experimental setup. EOM: electronic optical modulator; diagnostics: communication signal analyzer and autocorrelator.

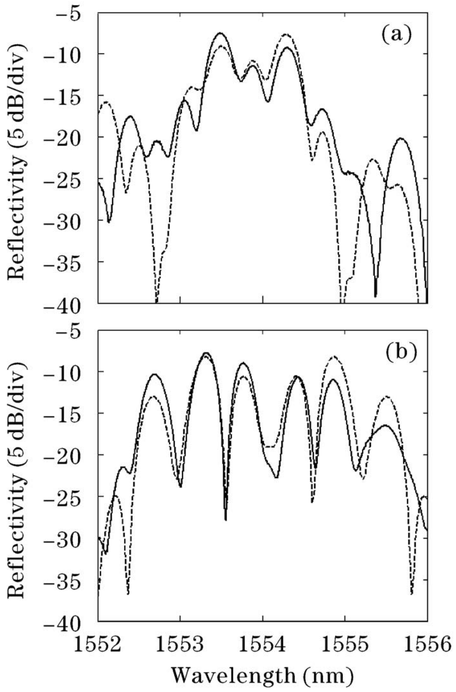

Fig. 2. Spectral reflectivity profiles of encoder grating Q_1 ($\pi/2$, $\pi/2$, 0, 0, $\pi/2$, π, $3\pi/2$) (a) and Q_2 (π, 0, 0, π, 0, π, π) (b) (solid curves: experiment; dashed curves: theory).

used to write the grating[7]. The 4-phase shift SSFBGs are fabricated using "equivalent phase shift" method[9], wherein the desired phase shift in one channel of sampled Bragg grating (SBG)[11] could be achieved by simply changing the sampling period. No special phase mask with desired phase shift or high precision control during fabrication is required, sub-micrometer precision in control is adequate in grating writing process. Compared with traditional methods[12,13], the equivalent phase shift method is markedly advantageous in the flexibility, repeatability, and cost-effectiveness in grating design and mass production, especially when multiple and mutable phase shifts are demand.

We performed encoding-decoding and associated transmission experiments at 40 Gb/s. Figures 3(a) — (c) show the degradation to the decoded signal traces as the number of OCDM channels is added into system compared with the original pulse trace. The pulse measurements were obtained using a fast diode and a scope with $\sim$ 10 ps resolution. The oscilloscope trace for the decoded pulse under matched case $Q_1 : Q_1^*$ is presented in Fig. 3(b), which clearly shows that short, distinct pulses are reformed. As can be seen by comparing the traces in Figs. 3(b) and (c), the effect of interchannel crosstalk is evident. The interference noise is primarily due to the temporal overlaps of two pseudo-orthogonal codes. Figure 3(d) shows trace for the decoded pulse under unmatched case $Q_2 : Q_1^*$, short pulses are not reformed.

We examined the decoded pulses using the second harmonic generation (SHG) intensity autocorrelator (< 100 fs resolution), in order to assess the duration of the resultant correlation signal. The results of SHG autocorrelation measurements of the pattern recognition pulse are shown in Fig. 4. The obtained trace is compared with theoretical intensity autocorrelation function of the

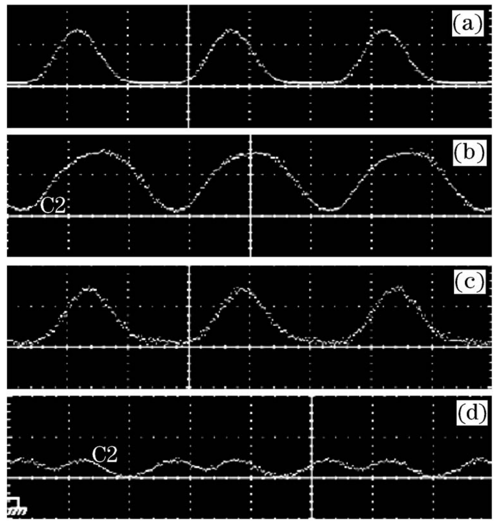

Fig. 3. Oscilloscope traces of incoming 1.3-ps pulse stream (a), decoded pulse ($Q_1 : Q_1^*$) (b), decode pulses ($Q_1+Q_2 : Q_1^*$) (c), and decode pulses (unmatched case: $Q_2 : Q_1^*$) (d) (detection bandwidth: $\sim$ 55 GHz, 10 ps/div).

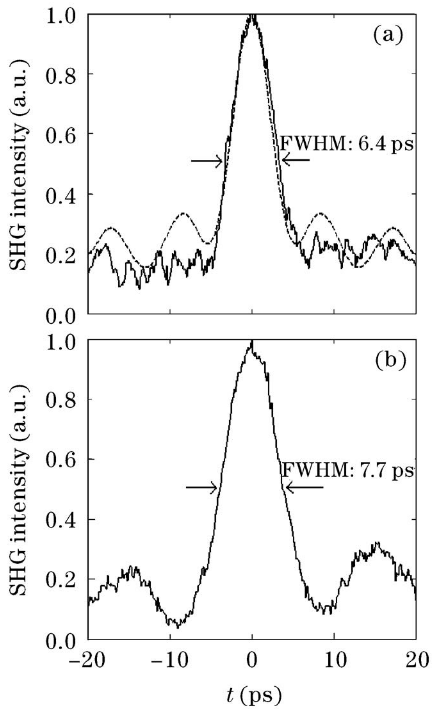

Fig. 4. Measured intensity autocorrelation traces of the decoded signals. (a) single channel ($Q_1 : Q_1^*$) (solid curve: experiment; dashed curve: theory). (b) 2-channel operation ($Q_1 + Q_2 : Q_1^*$).

decoded signal under single channel operation. The agreement between calculated trace and measured trace for the single channel encoding-decoding process $Q_1 : Q_1^*$ is seen to be excellent. We confirmed that the actual width of the peak for the process $Q_1 : Q_1^*$ was 6.4 ps, in good agreement with our theoretical calculation 5.9 ps.

There is evidence of some signal degradation in terms of the interchannel interference. However, a pulse with single, distinct peak was still obtained. The width of the main peak for 2-user operation $Q_1+Q_2 : Q_1^*$ is broadened to 7.7 ps (see Fig. 4(b)).

From a system perspective, it is essential that multichannel interference noise is minimized to as great an extent as possible. Improvement of the 40-Gb/s OCDM system performance needs further study. In order to multiplex added channels, ultrafast optical time-gating and optical hard thresholding are required to suppress the interference noise, and we are currently actively investigating this issue.

In conclusion, we have experimentally demonstrated 40-Gb/s quaternary phase encoding and decoding using SSFBGs. In addition, we have paid our attention to the deleterious impact of interchannel interference noise. The results highlight the precision and flexibility of "equivalent phase shift" method in grating writing process and show that SSFBG technology represents a promising technology for optical pulse processing. The high quality quaternary pulse encoding and decoding could find use in a variety of all optical network implementations, including both OCDM and packet switched networks.

The authors would like to thank Yitang Dai and Xiangfei Chen of Tsinghua University for their technical support in gratings fabricating process. This work was supported by the state "863" High Technology Program of China under Grant No. 2002AA122035. X. Chen's e-mail address is cxg826@yahoo.com.cn. D. Huang is the author to whom the correspondence should be addressed, his e-mail address is wnlo2@mail.hust.edu.cn.

References

1. K. Kitayama, H. Sotobayashi, and N. Wana, IEICE Trans. Fundam **E82-A,** 2616 (1999).
2. K. P. Jackson, S. A. Newton, B. Moslehi, M. Tur, C. C. Cutler, J. W. Goodman, and H. J. Shaw, IEEE Trans. Microwave Theory Tech. **33,** 193 (1985).
3. N. Wada and K. Kitayama, J. Lightwave Technol. **17,** 1758 (1999).
4. H. Tsuda, H. Takenouchi, T. Ishii, K. Okamoto, T. Goh, K. Sato, A. Hirano, T. Kurokawa, and C. Amand, Electron. Lett. **35,** 1186 (1999).
5. A. J. Jepson, A. Johnson, E. Maniloff, T. Mossberg, M. Munroe, and J. Sweetser, in *Proceeding of OFC'99* PD33-1 (1999).
6. X. Fang, S. Li, H. Tian, and D. Wang, Chin. Opt. Lett. **1,** 317 (2003).
7. P. C. Tech, P. Petropoulos, M. Ibsen, and D. J. Richardson, J. Lightwave Technol. **19,** 1352 (2001).
8. M. Ibsen, M. K. Durkin, M. J. Cole, M. N. Zervas, and R. I. Laming, in *Proceedings of IEE Colloquium on Optical Fibre Gratings 1999* 6/1 (1999).
9. Y. Dai, X. Chen, D. Jiang, S. Xie, and C. Fan, IEEE Photon. Technol. Lett. **16,** 2284 (2004).
10. S. Boztas, R. Hammons, and P. V. Kumar, IEEE Trans. Information Theory. **38,** 1101 (1992).
11. Y. Dai, X. Chen, L. Xia, Y. Zhang, and S. Xie, Opt. Lett. **29,** 1333 (2004).
12. R. Kashyap, P. F. McKee, and D. Armes, Electron. Lett. **30,** 1977 (1994).
13. W. H. Loh, M. J. Cole, M. N. Zervas, S. Barcelos, and R. I. Laming, Opt. Lett. **20,** 2051 (1995).